

# A global geomorphologic map of Saturn's moon Titan

R. M. C. Lopes<sup>1</sup>\*, M. J. Malaska<sup>1</sup>, A. M. Schoenfeld<sup>2</sup>, A. Solomonidou<sup>3</sup>, S. P. D. Birch<sup>4</sup>, M. Florence<sup>1</sup>, A. G. Hayes<sup>4</sup>, D. A. Williams<sup>5</sup>, J. Radebaugh<sup>6</sup>, T. Verlander<sup>7</sup>, E. P. Turtle<sup>8</sup>, A. Le Gall<sup>9</sup> and S. D. Wall<sup>1</sup>

**Titan has an active methane-based hydrologic cycle<sup>1</sup> that has shaped a complex geologic landscape<sup>2</sup>, making its surface one of most geologically diverse in the Solar System. Despite the differences in materials, temperatures and gravity fields between Earth and Titan, many of their surface features are similar and can be interpreted as products of the same geologic processes<sup>3</sup>. However, Titan's thick and hazy atmosphere has hindered the identification of its geologic features at visible wavelengths and the study of its surface composition<sup>4</sup>. Here we identify and map the major geological units on Titan's surface using radar and infrared data from the Cassini orbiter spacecraft. Correlations between datasets enabled us to produce a global map even where datasets were incomplete. The spatial and superposition relations between major geological units reveals the likely temporal evolution of the landscape and provides insight into the interacting processes driving its evolution. We extract the relative dating of the various geological units by observing their spatial superposition in order to get information on the temporal evolution of the landscape. The dunes and lakes are relatively young, whereas the hummocky or mountainous terrains are the oldest on Titan. Our results also show that Titan's surface is dominated by sedimentary or depositional processes with a clear latitudinal variation, with dunes at the equator, plains at mid-latitudes and labyrinth terrains and lakes at the poles.**

Titan's surface has been modified by several geological processes, including impact cratering<sup>5,6</sup>, fluvial or aeolian erosion and deposition<sup>7–11</sup>, precipitation<sup>12</sup>, dissolution<sup>13</sup>, tectonism<sup>14</sup> and possibly cryovolcanism<sup>15</sup>. Data returned by the Cassini spacecraft have also revealed Titan to be a world rich in organic materials<sup>9,16</sup>, which mantle the surface to a depth of at least several tens of centimetres in most places<sup>17</sup>. These materials are eroded, transported and deposited across the landscape<sup>9,18</sup>. Geological mapping can place Titan's terrain types in stratigraphic order<sup>2,3,19</sup>, constraining the relative importance and global distribution of various endogenic and exogenic processes<sup>2</sup>.

The dataset best suited for interpreting Titan's surface geology from orbit was obtained using synthetic aperture radar (SAR) from Cassini, as Titan's hazy atmosphere limits the signal-to-noise ratio of visible and near-infrared observations but is transparent to the radar's operating wavelength of 2.17 cm ( $K_u$  band). On the SAR images, we defined six major geological units (based primarily on backscatter and overall morphology, as done for prior mapping<sup>2,3</sup>)

as follows: plains, dunes, hummocky terrain, lakes, labyrinth terrain and craters (Fig. 1). Mapping the distribution of these units enables us to discern their latitudinal distribution, superposition relations, composition and areal coverage, and the implications for Titan's geological history. We first mapped the areas covered by SAR (about 46% of Titan's surface at less than 1 km resolution). We then used correlations between SAR and other datasets—obtained using

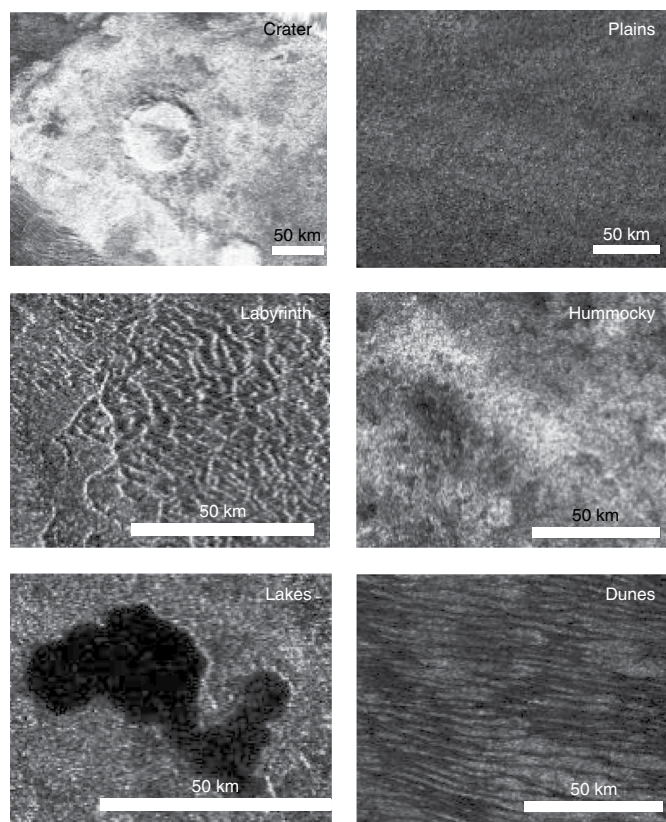


**Fig. 1 | SAR images showing examples of the main classes of geomorphologic units on Titan.** Scale bars are 50 km, with global area percentages covered by each major unit provided below.

<sup>1</sup>Jet Propulsion Laboratory, California Institute of Technology, Pasadena, CA, USA. <sup>2</sup>UCLA Department of Earth, Planetary, and Space Sciences, Los Angeles, CA, USA. <sup>3</sup>European Space Agency (ESA), ESAC, Madrid, Spain. <sup>4</sup>Department of Astronomy, Cornell University, Ithaca, NY, USA. <sup>5</sup>Arizona State University, Tempe, AZ, USA. <sup>6</sup>Department of Geological Sciences, Brigham Young University, Provo, UT, USA. <sup>7</sup>University of Oklahoma, School of Civil Engineering and Environmental Science, Norman, Oklahoma, USA. <sup>8</sup>JHU Applied Physics Lab, Laurel, MD, USA. <sup>9</sup>LATMOS/IPSL, UVSQ Université Paris-Saclay, UPMC Université Paris 06, CNRS, Guyancourt, France. \*e-mail: [rosaly.m.lopes@jpl.caltech.edu](mailto:rosaly.m.lopes@jpl.caltech.edu)

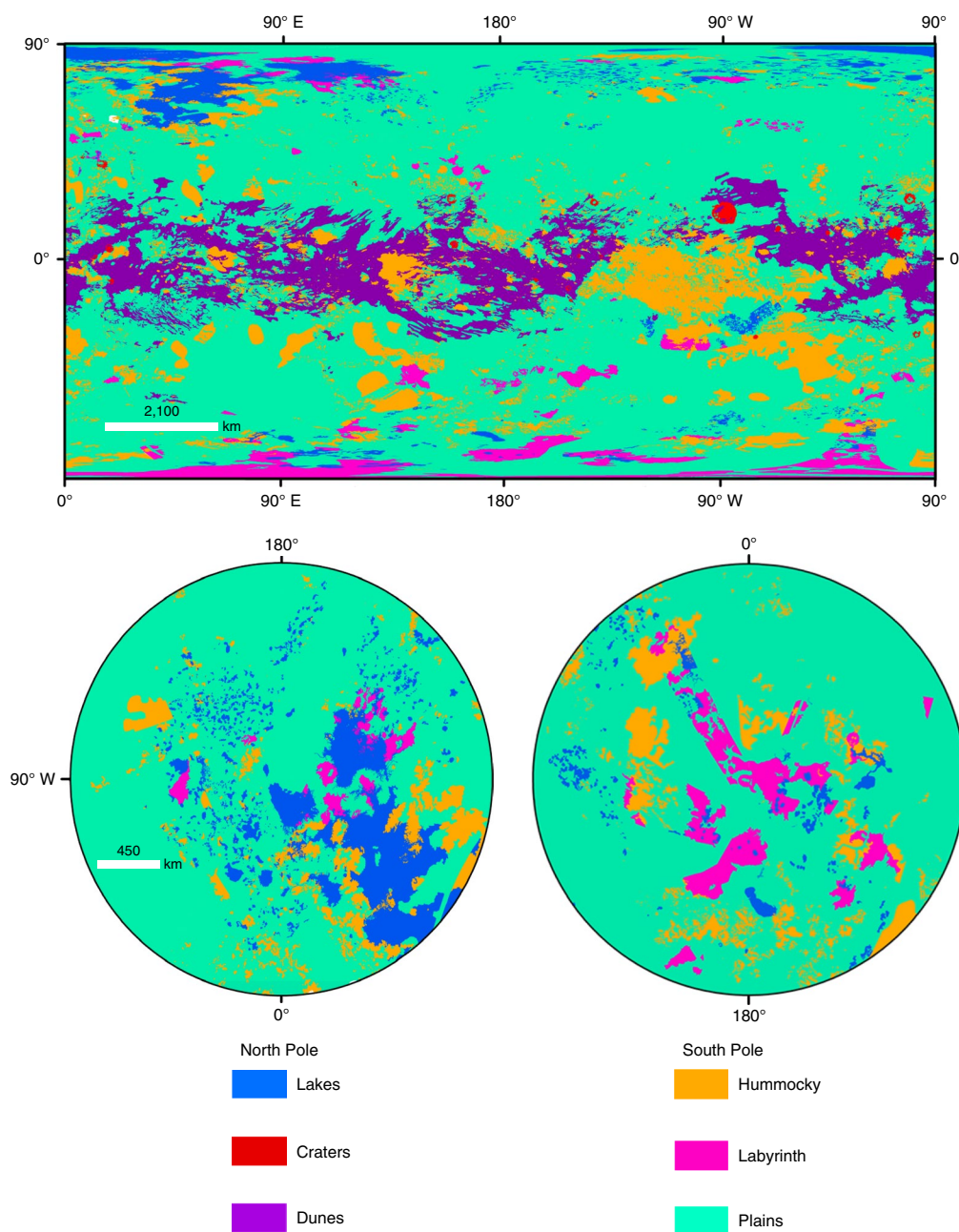


**Fig. 2 | Global map of Titan's major geomorphological units.** The map projections are Mercator (top) and polar stereographic (bottom, for  $>55^\circ$  N and  $^\circ$ S).

low-resolution, high-altitude SAR, radiometry, the Imaging Science Subsystem (ISS) and the Visible and Infrared Mapping Spectrometer (VIMS)—to extend the mapping to regions not covered by SAR (see Methods), finally producing a global 1:20,000,000 scale map of the major geological units (Fig. 2). This scale is appropriate for defining the six major units we present in this paper, although it is coarser than the 1:800,000 scale maps done for individual regions such as that of the Afekan crater<sup>3</sup>. The main difference between the 1:800,000 scale map and the 1:20,000,000 scale maps is that the sub-units in the finer-scale map do not appear in the 1:20,000,000 map (Fig. 3). Correlations between these datasets enabled us to map the global geology even where datasets were incomplete and to place geomorphological units in relative stratigraphic and areal context to provide a sequence of events for the surface evolution of Titan.

The majority of Titan's surface is comprised of plains, which make up 61% of the SAR-imaged areas and 65% of the global area

(Table 1). Several types of plain were mapped at a regional scale (see Methods), the most extensive of which are the undifferentiated plains, which appear near-uniform and radar-dark in SAR images, lacking major topographical relief<sup>11</sup>. The lack of fluvial features in this terrain unit at Cassini SAR scale suggests that it is porous, is not able to support large, integrated channels or that it has buried and reworked older, extinct channel networks<sup>10</sup>. Plains dominate Titan's mid-latitudes and show high emissivity to radar, consistent with organic materials<sup>17</sup>. Previous work<sup>11</sup> argued that undifferentiated plains are depositional or sedimentary in nature, perhaps with aeolian deposition being the major process contributing to their formation. However, latitudinal variations exist. Analyses of VIMS data show that plains closer to the equator, and therefore closest to the largest dune fields, have spectral similarities to dune materials<sup>4,11</sup>, suggesting that some contamination by dune material was probably transported into the plains by wind. The high-latitude



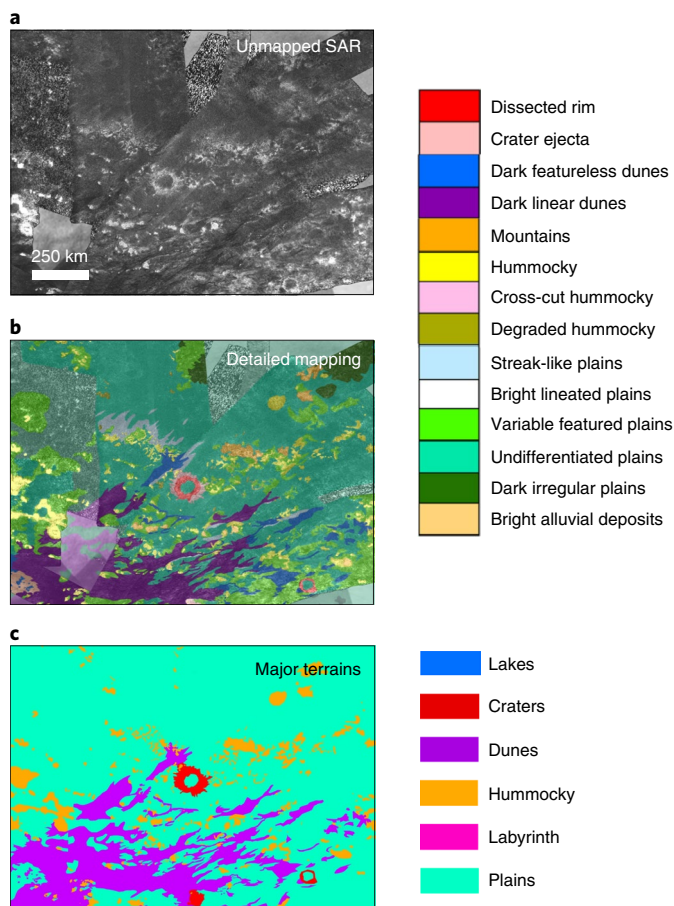


**Fig. 3 | Example of the mapping method from regional to global.**

**a**, Unmapped SAR data over ISS data. **b**, Detailed mapping over SAR (at 1:800,000 scale) and mapping of areas covered by ISS and other datasets but not SAR (pale colours). **c**, Major terrains. The colours correspond to the detailed mapping of terrains and the major units for the 1:20,000,000 scale map.

VIMS spectra are consistent with an unknown material that is also observed in the labyrinth unit<sup>1</sup>.

Dunes (comprising both dunes and interdunes) dominate the equatorial regions ( $\pm 30^\circ$  latitude) and make up the second-most extensive unit on Titan by areal coverage, 19% of the SAR-imaged area and 17% of the global area. Dunes appear as long, narrow, SAR-dark features, indicating that dune materials are smooth or absorbing at 2.17 cm. Previous measurements show that dunes are mostly 1–2 km wide, spaced by 1–4 km and can be hundreds of kilometres long<sup>9</sup>. Limited measurements of heights suggest that the dunes are 80–130 m tall<sup>20</sup>. The general direction of transport of sand (west to east) has been inferred from the way dunes interact with topographic obstacles, such as hummocky and mountainous terrain<sup>18,21</sup>. Their large-scale morphology and sizes are similar to those of linear sand dunes on Earth<sup>21</sup>. Dunes show high emissivity to radar, consistent with organic materials<sup>17</sup>.

The hummocky unit consists of mountain chains and isolated terrains that are topographically higher than the surrounding areas<sup>18</sup>. This unit covers 15% of the SAR-imaged surface and 14% of the global area. Hummocky terrains appear bright in SAR images because of the roughness and fractured nature of the materials<sup>17</sup>, as well as the terrain topography with respect to the SAR look direction and incidence angle (typically tens of degrees). They are characterized by high scattering and low emissivity in the radiometry mode<sup>17</sup>, indicating water-ice materials that increase the likelihood

**Table 1 | Percentage of the total area on Titan covered by each of the main classes of geomorphological unit**

Plains	65%
Dunes	17%
Hummocky	14%
Lakes	1.5%
Labyrinth	1.5%
Crater	0.4%

of volume scattering. The largest areal exposure of the hummocky unit is in the equatorial region known as Xanadu<sup>22,23</sup>. Elsewhere, hummocky materials are exposed as locally isolated peaks or ranges (generally under 30 km<sup>2</sup>). Mountains are mostly exposed as gently undulating regions from mid- to high latitudes, generally aligned east-to-west, and may have formed by contractional tectonism<sup>14</sup> early in Titan's history. They are a few to tens of kilometres in length and up to a couple of kilometres high above the reference geoid. Analyses of VIMS data for the hummocky unit indicate a relatively high water-ice component<sup>22</sup>. Derived surface albedos of some small exposures of hummocky terrains (not within Xanadu) suggest that the hummocky unit is relatively dark, containing a spectrally dark constituent<sup>19</sup> in addition to water ice in the mixture; other VIMS results<sup>22</sup> suggest differences between Xanadu and other hummocky terrains. These results are consistent with the hummocky unit representing exposed remnants of Titan's icy shell<sup>2</sup>, in parts covered in a sedimentary veil of organics originating in Titan's atmosphere.

The lakes unit comprises lakes and seas, which can either be dry or liquid-filled. Titan's polar regions contain over 650 lakes<sup>19</sup>, either dry or filled with liquid hydrocarbons. The majority of filled lakes and seas (maria) are located in the north polar region, mostly (approximately 80%) in the Kraken, Ligeia and Punga maria. These larger northern maria have varied shorelines indicating flooding and draining of pre-existing topography, whereas the majority of the smaller lakes form steep-sided depressions with no true terrestrial analogue<sup>24</sup>. In the south, Ontario Lacus appears as a residual lake inset in a larger palaeobasin. The morphologies of both dry and filled lakes and seas on Titan may provide a record of past and current climatic conditions and surface evolution processes<sup>25,26</sup>. The lakes unit makes up only 2.2% of the SAR-imaged areas and 1.5% of Titan's total surface area.

The labyrinth unit consists of terrains with medium SAR backscatter and the appearance of being highly incised and dissected plateaus. These terrains cover 2.1% of the SAR-imaged area and 1.5% of the global area, and are primarily located at high latitudes. Topographic data indicate that this unit is locally elevated. VIMS data of the top surface are consistent with a material compatible with hydroxide-bearing constituent (this spectral response has been ascribed to water ice<sup>9</sup>). Fluvial valley networks (rectangular to dendritic) inside the labyrinth units suggest some structural and topographic control. Radiometry data show that, like dune materials, this unit has high emissivity, consistent with materials that are organic in composition and thus have a low bulk dielectric constant. Labyrinths have morphologies similar to karstic terrain and may have formed through a combination of dissolution, possibly karstic<sup>9</sup>, coupled with mechanical erosion, or other processes or phase changes that could allow the formation of closed valleys (at least at the SAR resolution) and transport of materials to the surrounding plains.

Craters occupy only 0.7% of Titan's SAR-imaged area and 0.4% of the global area. Only 23 craters more than 20 km in diameter were identified with a high degree of certainty (plus about ten others as probable) from all datasets, plus a few smaller crater candidates<sup>27</sup>. This suggests that Titan has a crater retention age of several

hundred million years<sup>5</sup>. The distribution of craters also shows some latitudinal variation, consistent with the oldest exposed surfaces being located near the equator and the youngest surfaces located near the poles<sup>27</sup>, where there is an almost complete absence of craters. Most craters show evidence of erosion by aeolian and fluvial or pluvial processes. The absence of craters in the polar regions could be due to infilling of the polar basins by sediments<sup>19</sup>, increased erosion by fluvial processes<sup>27</sup> or impacts into former marine environments<sup>28</sup>. The microwave emissivity of the less-degraded crater rims and ejecta is among the lowest on Titan<sup>17</sup>, consistent with icy materials excavated by the impact. The inferred composition from radar and VIMS data is crustal water ice or a mixture of crustal water ice and organic materials<sup>6</sup>.

The scarcity of craters on Titan limits the viability of crater counting statistics for distinguishing the ages of different terrains. However, contacts between units and superposition relations can be used to infer their relative ages. Contacts mapped from the complete SAR dataset confirm early suggestions<sup>2</sup> that the oldest units on Titan are the hummocky terrains (including mountains). The plains are younger than both the hummocky and labyrinth units. Dunes and lakes (including seas) are the youngest units on Titan<sup>2,3,21</sup>. Because there is no contact between lakes and dunes, it is not possible to distinguish the relative ages of these units and, given active seasonal weather patterns including rainfall<sup>12</sup> and wind<sup>29</sup>, it is likely that both lakes and dunes are still forming and changing on Titan. Craters are an intermediate unit in relative age, with some seen in hummocky terrain, particularly in the Xanadu area, and several infilled by dune and plains materials.

The resulting global-scale geologic map shows a clear latitudinal dependence of the major units. Equatorial regions are dominated by vast dune fields and the mid-latitudes are dominated by plains, while the lakes and labyrinth units are found primarily in the polar regions. This may be related to more humid conditions in the polar regions. Superimposed on top of the global latitudinal unit distribution is a dichotomy in liquid inventories between north and south. The vast majority of filled lakes is currently situated in the northern hemisphere, while the south is nearly dry, possibly the result of global climate cycles<sup>19,25</sup>. The hummocky unit, interpreted as exposed crustal materials, is seen at all latitudes, but primarily in the equatorial Xanadu region, for reasons yet unknown<sup>23</sup>.

In terms of composition, the emissivity data are consistent with organic materials forming the plains, dunes, lakes and labyrinth units, while the emissivity of the crater and hummocky units indicates a higher abundance of water-ice materials<sup>17,30</sup>. This suggestion that the latter terrains expose icy crustal material is consistent with previous work that predicted and later showed<sup>16</sup> that organic materials produced by high-altitude photochemistry of methane and nitrogen in Titan's atmosphere form a surficial unit that covers much of Titan's surface. Relative ages and distribution of the major units imply that Titan's old, icy crust (hummocky materials) has been covered by sedimentary materials like the dunes and plains, particularly at lower latitudes, with the exception of Xanadu. In the polar regions, where cumulative rainfall outpaces infiltration or evaporation of liquids, lakes are abundant. Labyrinth terrains, which are older than plains and mostly located at higher latitudes, may have begun as uplifted or otherwise elevated terrains, predominantly of organic deposits, that later became heavily incised and dissolved by rainfall, like karstic formations on Earth.

Titan is covered by organic sediments that are reworked, to varying degrees, by aeolian, pluvial and fluvial processes. Though rainfall occurs at all latitudes, Titan's equatorial climate is arid over long enough timescales that aeolian deposition and dune formation dominate. Towards the poles, relative humidity increases, and liquid hydrocarbon lakes and seas dominate the polar landscape. Between these two extremes is a vast area of mid-latitude, featureless, organic plains. The clear distinction between these units and where they are

found on Titan indicates that a variety of processes must be acting on the surface of this moon, controlled by climatic, seasonal and elevational conditions.

## Methods

Titan's hazy atmosphere scatters light at visual to near-infrared wavelengths, limiting the detailed visual and infrared spectroscopy data that can constrain surface composition. Longer-wavelength microwave radiation, however, penetrates the atmosphere and interacts with the surface with no significant atmospheric interference. We primarily used data from the Cassini RADAR instrument in its Synthetic Aperture Radar (SAR) mode to map Titan's geology, following methodology outlined in previous work<sup>2,3,31</sup>. SAR data respond to near-surface roughness at the wavelength scale (2.17 cm), to surface slopes at the pixel scale, and to near-surface dielectric properties of the materials. SAR can penetrate many wavelengths into some materials as well<sup>17</sup>. Global maps by ISS<sup>32,33</sup> (at 0.938  $\mu\text{m}$ ) and VIMS<sup>34–36</sup> (1–5  $\mu\text{m}$ ) are helpful in unit characterization and global distribution; they provide a complementary dataset that is sensitive to the top surface coating on the order of tens of micrometres, while microwave emissivity penetrates tens of centimetres into the surface<sup>17</sup>. Furthermore, analysis and interpretation of VIMS data provide information on the spectral nature and chemical composition of the surface<sup>4</sup>. Terrain units have therefore been characterized in terms of radar backscatter, morphology, contact relations, internal texture, topographic relationships and observed characteristics (ISS, VIMS, and radiometry), following the method outlined in previous work<sup>3</sup>.

The Cassini RADAR instrument<sup>37</sup> operates in four modes: SAR, altimetry, scatterometry and radiometry. The SAR mode was mostly used at spacecraft altitudes under approximately 5,000 km, imaging Titan's surface at incidence angles of 15–35°. The data yielded images with spatial resolution from around 350 m to 1.5 km, sufficient to identify major terrains for geological maps<sup>31</sup>. During each Titan encounter with SAR imaging, a swath 120–450 km in width and 1,000–5,000 km in length was created from five antenna beams, with coverage largely determined by spacecraft range and orbital geometry. SAR data (in nominal mode) cover about 46% of Titan's surface at less than 1 km resolution, while the higher-altitude SAR data cover an additional 24% at less than 5 km resolution. The SAR dataset was used as a basemap for our geomorphological mapping. We used SAR data to define the boundaries of the terrain contacts and the main units, but data from other radar modes and other instruments were important as supplementary datasets, particularly in areas where SAR was not available. Topographic data were obtained from the SAR swaths by SARTopo<sup>38</sup> and in some other locations by using the RADAR in altimetry mode. The RADAR radiometry mode provided a global map of microwave emissivity<sup>17</sup>. With the use of specific tools, the analysis and interpretation of VIMS data can provide useful information on the spectral nature and chemical composition of the surface<sup>4</sup>. The terrain units were therefore characterized in terms of SAR backscatter, morphology, contact relations, internal texture, topographic relationship and observed characteristics in ISS, VIMS and radiometry, following the method previously outlined<sup>3</sup>.

Global coverage of the surface was acquired by ISS, VIMS and RADAR radiometry, with variable spatial resolution. The characteristics of each unit in the different datasets provide other information and can be used to infer the main type of unit in areas not imaged by SAR. We removed areas too small to be observed at the 1:20,000,000 scale (approximately areas less than 30 km<sup>2</sup> in spatial extent). For example, the crater subunits in the 1:800,000 scale regional maps (crater rim, crater ejecta, central peak, crater fill shown in Fig. 3) were simply mapped as the crater unit in the 1:20,000,000 scale global map. Likewise, areas showing linear dunes and dark areas interpreted as featureless sand sheets were mapped as the dune unit; filled and empty lakes and seas were mapped as the lake unit; hummocky, mountainous and degraded mountain subunits were mapped as hummocky; and plains subunits (undifferentiated, streak-like, variable featured, dark irregular, scalloped and bright gradational) were mapped as plains. Detailed discussions of these different terrains are given in a previous work<sup>3</sup>.

The mapping was done using ArcGIS (ESRI) software (<https://www.esri.com/en-us/arcgis/about-arcgis/overview>). Starting with the SAR-imaged areas, we identified contacts between regions based on radar backscatter and gross geomorphology<sup>2,3</sup>. These were then used to build polygons with attribute tables describing the units. The units used the geometry of the contacts, sharpness of contact, internal texture, channel density and sinuosity, degree of dissection, preferred orientation of diagnostic features or contacts and overall morphology. Data from the other radar modes and instruments were used to further characterize each unit<sup>3</sup>. Crosscutting and superposition relations were used to determine relative stratigraphy, and the available topographic data were used to confirm the stratigraphic sequence among the terrain units. The plains units are extensive and appear continuous in many areas. More importantly, the plains unit shows a direct contact with all other terrain units mapped. Therefore, the plains unit was used to determine embayment and superposition relations with other units, from which relative ages could be inferred, with the caveat that exposures of the plains units may not have been formed at the same time in the same location<sup>3</sup>. Although all units were in contact with the plains, some units were not in contact with each other, so a stratigraphic sequence could not be determined for them.

For example, direct contacts were not observed between hummocky and labyrinth units, but both were observed to have been superposed by plains (and must therefore be older).

We used correlations obtained from the SAR mapping with the other datasets to extend the mapping to the areas not imaged by SAR. For these areas, we used the global datasets from ISS, VIMS, radiometry and, where available, high-altitude SAR and topographic information from altimetry and SARTopo<sup>38</sup>. For example, undifferentiated plains appear bland and dark in SAR and high-altitude SAR but bright in ISS and have high emissivity in radiometry<sup>11</sup>. Correlations across several datasets have been discussed in detail in several published papers<sup>3,4,11</sup>. An example of mapping is shown in Fig. 3. Because the non-SAR areas were mapped at a much lower resolution than the SAR area, they are already at a scale appropriate to be included in the 1:20,000,000 scale global map. Below we describe the subunits within each of our major units.

**Plains.** Plains were classified into several subunits<sup>3</sup>, but undifferentiated plains<sup>11</sup> are by far the most extensive on Titan. They are low-backscatter regions that appear largely uniform in SAR data, having only a few (<5% by surficial area) observable features at the mapping scale of 1:800,000. Topographically, there is some variation in relief across the undifferentiated plains, but they are lower in local elevation than the hummocky unit. These terrains appear bright in ISS data. The same is true for VIMS data for the undifferentiated plains located in the high latitudes. Much smaller patches of other types of plain have been identified in our 1:800,000 scale regional mapping, generally at mid- to high latitudes. They are divided into bright lineated plains, bright streak-like plains, variable-featured plains, dark irregular plains and scalloped plains<sup>3</sup>. Both types of bright plain are interpreted as aeolian-dominated landscapes consisting of high-backscatter materials. Variable-featured plains are interpreted to result from erosion of hummocky terrains, possibly involving fluvial erosion and deposition. Dark irregular plains are topographically lower than surrounding terrains, interpreted as areas dampened by liquid hydrocarbons, or lowland muds (within the top tens of centimetres of the surface). Scalloped plains are interpreted as eroded hummocky terrains with a cover of organic materials not thick enough to mask their nature. Scalloped plains may be transitional between hummocky terrains and undifferentiated plains. All the plains are mapped as a single unit in the 1:20,000,000 scale global map.

**Dunes.** These areas were mapped at the regional 1:800,000 scale as three subunits: linear dunes, reticulated dunes and featureless dune sands<sup>3</sup>. The linear dunes subunit shows characteristic dune lineations in the SAR image across most of the areal extent of the terrain unit, whereas the featureless sand sheets contain only a few extended broad lanes that can be discerned in select areas. Both types of terrains are interpreted as deposits composed of sand-sized grains<sup>9</sup> that form linear dunes that are located generally at lower latitudes. Reticulated dunes are small patches of linear dunes showing a pattern perpendicular to the orientation of linear dunes nearby. These areas are interpreted as regions where the wind field is varying and the deposition therefore occurs in a more complex pattern than those that generate linear dunes. Dunes appear dark in both ISS and SAR, have high emissivity in microwave radiometry measurements consistent with organic materials, and correspond to the VIMS 'dark brown unit' in 3-band VIMS global maps<sup>39,40</sup>. Radiative transfer analysis of VIMS data from various dune fields showed (generally including both dune and interdune features where the resolution limit prevents VIMS from distinguishing between the two) that the dunes are spectrally flat and very dark in the VIMS range<sup>4</sup>. In the 1:20,000,000 scale map, all the dune subunits were mapped as dunes.

**Hummocky.** This unit consists of four subunits previously described<sup>3</sup> as hummocky, mountains, degraded hummocky and cross-cut hummocky. All are areas of high SAR backscatter and show locally positive topographic expression. The main difference between mountains and hummocky subunits is that the mountains appear elongated in shape and show RADAR uprange-to-downrange bright-to-dark pairing, whereas the hummocky unit shows uniform to grainy internal textures. Degraded hummocky are small (<5 km across) and generally found in plains. Cross-cut hummocky terrains are larger (>100 km in diameter) and cut by linear features, possibly graben. All subunits of hummocky terrains appear bright in ISS images. The microwave radiometric response for all these subunits indicates that they are composed of fractured water ice or mixtures of fractured water ice and organic materials<sup>17</sup>, and these areas are interpreted as exposures of ancient crust or bedrock, consistent with the interpretation of the hummocky or mountainous unit previously proposed<sup>3</sup>.

**Lakes.** We mapped both filled and empty lakes following criteria discussed in previous work<sup>19</sup>. Filled lakes are generally radar dark, although their darkness varies as a function of their fill state. Owing to the transparency of liquid methane to Cassini's RADAR<sup>41</sup>, all the filled liquid bodies mapped by SAR are at least a few metres deep. The filled lakes and seas are also clearly seen in ISS and VIMS images, allowing for an accurate assessment of lake/sea surface areas in areas not imaged by SAR. Empty lakes appear similar in planform to the filled lakes, because they form closed topographic lows<sup>19,42</sup>. Their perimeters form steep-sided walls, with a distinct curvature that indicates expansion by uniform scarp retreat<sup>24</sup>.

They have a variety of radar appearances, however, with some appearing radar-bright relative to their surroundings, while others do not. In all cases, empty lakes are morphologically distinct features that are recognizable at the 1:800,000 scale. At both poles, lakes (either empty or filled) always appear in clusters, while the seas occupy topographic lows. The total number of filled or empty lakes is similar at both poles<sup>19</sup>, but 97% of Titan's liquids (by area) reside in the north polar region, with only nine filled lakes observed in the south.

**Labyrinth.** All the labyrinth terrains are mapped as one unit in both the regional and global maps, although variations exist in terms of width of valleys and intervening ridge spacing. This unit appears to be highly dissected, with a clear uprange-to-downrange bright-to-dark pairing<sup>3</sup> in SAR images, representing plateaus with valleys containing fill material that appears dark in SAR. The labyrinth unit shows overall medium radar backscatter and exposures are generally more than 5,000 km<sup>2</sup> in extent. Topographic data show that labyrinths are locally elevated. Valley and ridge widths are variable, in areas where the valleys are wide (>2 km) and the exposures of elevated terrain are narrow (<2 km), the area appearance is of a series of remnant ridges. In contrast, where the valleys are narrow (<2 km) and the intervening elevated terrains are wide (>2 km), the area can appear as highly dissected plateaus. ISS and VIMS data show the labyrinth unit to be slightly darker in the near-infrared than the surrounding plains<sup>3,43</sup>. The labyrinth unit is interpreted as dissected plateaus and remnant ridges of organic materials that then transport plains materials into the valleys and downstream basins<sup>3</sup>. Undifferentiated plains are often found in the valleys as fill and at the distal edges of the valleys, suggesting that the labyrinth terrains may be plateaus composed of undifferentiated plains materials.

**Crater.** The overall morphologic expression of a Titan crater is a partial or complete circle of high SAR backscatter materials. Craters can be easily identified if they are larger than several tens of kilometres in diameter. Impact craters and ejecta can often be identified in VIMS and ISS images<sup>6</sup>. The challenge of identifying partial circular features as craters has been previously described<sup>3,44</sup>. We cross-checked our crater identifications with previous mappings<sup>3,44</sup> and found agreement in all but a few cases where identification was subjective, generally because of rim erosion and no discernible ejecta. Craters may be surrounded by an extended region of crater ejecta, plains or other near-infrared-bright units; these terrains often extend in the inferred downwind direction (eastward)<sup>3</sup>. In a few craters, a central peak is observed at the centre (or inferred centre) of the circular rim. The margins of the crater rim may have become dissected by fluvial erosion or mass-wasting processes<sup>45</sup>. Ejecta may be covered over by plains materials, which are also seen inside several of the craters, interpreted as wind-blown deposits<sup>11</sup>.

## Data availability

The Cassini data used in this paper are available from NASA's Planetary Data System (PDS) (<https://pds.nasa.gov>). Data on map units are available from the corresponding author upon reasonable request.

Received: 3 January 2019; Accepted: 13 September 2019;  
Published online: 18 November 2019

## References

- Hayes, A. G., Lunine, J. I. & Lorenz, R. D. Titan's hydrologic cycle: a post-Cassini view. *Nat. Geosci.* **11**, 306–313 (2018).
- Lopes, R. M. C. et al. Distribution and interplay of geologic processes on Titan from Cassini RADAR data. *Icarus* **205**, 540–588 (2010).
- Malaska, M. J. et al. Geomorphological map of the Afekan Crater region, Titan: terrain relationships in the equatorial and mid-latitude regions. *Icarus* **270**, 130–161 (2016).
- Solomonidou, A. et al. The spectral nature of Titan's major geomorphological units: constraints on surface composition. *J. Geophys. Res. Planet* **123**, 489–507 (2018).
- Wood, C. A. et al. Impact craters on Titan. *Icarus* **206**, 334–344 (2010).
- Neish, C. D. et al. Spectral properties of Titan's impact craters imply chemical weathering of its surface. *Geophys. Res. Lett.* **42**, 3746–3754 (2015).
- Burr, D. M., Emery, J. P., Lorenz, R. D., Collins, G. C. & Carling, P. A. Sediment transport by liquid surficial flow: application to Titan. *Icarus* **181**, 235–242 (2006).
- Lorenz, R. D. et al. Fluvial channels on Titan: initial Cassini RADAR observations. *Planet. Space Sci.* **56**, 1132–1144 (2008).
- Lorenz, R. D. et al. The sand seas of Titan: Cassini RADAR observations of longitudinal dunes. *Science* **312**, 724–727 (2006).
- Radebaugh, J. et al. Alluvial and fluvial fans on Saturn's moon Titan reveal processes, materials and regional geology. In *Geology and Geomorphology of Alluvial and Fluvial Fans: Terrestrial and Planetary Perspectives* (eds Ventra, D. & Clarke, L. E.) (Geol. Soc. Lond. Spec. Publ. 440, 2016).
- Lopes, R. M. C. et al. Nature, distribution, and origin of Titan's undifferentiated plains ("blandlands"). *Icarus* **270**, 162–182 (2016).



12. Turtle, E. P. et al. Rapid and extensive surface changes near Titan's equator: evidence of April showers. *Science* **331**, 1414–1417 (2011).
13. Cornet, T. et al. Dissolution on Titan and on Earth: toward the age of Titan's karstic landscapes. *J. Geophys. Res. Planets* **120**, 1044–1074 (2015).
14. Mitri, G. et al. Mountains on Titan: modeling and observations. *J. Geophys. Res.* **115**, E10 (2010).
15. Lopes, R. M. C. et al. Cryovolcanism on Titan: new results from Cassini RADAR and VIMS. *J. Geophys. Res. Planets* **118**, 1–20 (2013).
16. Clark, R. N. et al. Detection and mapping of hydrocarbon deposits on Titan. *J. Geophys. Res. Planets* **115**, (2010).
17. Janssen, M. A. et al. Titan's surface at 2.18-cm wavelength imaged by the Cassini RADAR radiometer: results and interpretations through the first ten years of observation. *Icarus* **270**, 443–459 (2016).
18. Malaska, M. J. et al. Material transport map of Titan: the fate of dunes. *Icarus* **270**, 183–196 (2016).
19. Birch, S. P. D. et al. Geomorphologic mapping of Titan's polar terrains: constraining surface processes and landscape evolution. *Icarus* **282**, 1–23 (2017).
20. Neish, C. D. et al. Radarclinometry of the sand seas of Africa's Namibia and Saturn's moon Titan. *Icarus* **208**, 385–394 (2010).
21. Radebaugh, J. et al. Linear dunes on Titan and Earth: initial remote sensing comparisons. *Geomorphology* **121**, 122–132 (2010).
22. Barnes, J. W. et al. Near-infrared spectral mapping of Titan's mountains and channels. *J. Geophys. Res. Planets* **112**, E11006 (2007).
23. Radebaugh, J. et al. Regional geomorphology and history of Titan's Xanadu province. *Icarus* **211**, 672–685 (2011).
24. Hayes, A. G. et al. Topographic constraints on the evolution and connectivity of Titan's lacustrine basins. *Geophys. Res. Lett.* **44**, 11745–11753 (2017).
25. Birch, S. P. D. et al. Morphological evidence that Titan's southern hemisphere basins are paleoseas. *Icarus* **310**, 140–148 (2018).
26. Turtle, E. P. et al. Titan's meteorology: evidence for extensive subsurface methane reservoirs. *Geophys. Res. Lett.* **45**, 5320–5328 (2018).
27. Neish, C. D. et al. Fluvial erosion as a mechanism for crater modification on Titan. *Icarus* **270**, 114–129 (2016).
28. Neish, C. D. & Lorenz, R. D. Elevation distribution of Titan's craters suggests extensive wetlands. *Icarus* **228**, 27–34 (2014).
29. Rodriguez, S. et al. Observational evidence for active dust storms on Titan at equinox. *Nat. Geosci.* **11**, 727–732 (2018).
30. Griffith, C. A. et al. A corridor of exposed ice-rich bedrock across Titan's tropical region. *Nat. Astron.* **3**, 642–648 (2019).
31. Williams, D. et al. Geologic mapping of the Menrva region of Titan using Cassini RADAR data. *Icarus* **212**, 744–750 (2011).
32. Porco, C. C. et al. Cassini imaging science: instrument characteristics and anticipated scientific investigations at Saturn. *Space Sci. Rev.* **115**, 363–497 (2004).
33. Karkoschka, E. et al. A global mosaic of Titan's surface albedo using Cassini images. In *Division for Planetary Sciences 50th Meeting* 216.02 (American Astronomical Society, 2018).
34. Brown, R. H. et al. The Cassini Visual and Infrared Mapping Spectrometer (VIMS) investigation. *Space Sci. Rev.* **115**, 111–168 (2004).
35. Le Mouélic, S. et al. The Cassini VIMS archive of Titan: from browse products to global infrared color maps. *Icarus* **319**, 121–132 (2019).
36. Le Mouélic, S. et al. Global mapping of Titan's surface using an empirical processing method for the atmospheric and photometric correction of Cassini/VIMS images. *Planet. Space Sci.* **73**, 178–190 (2012).
37. Elachi, C. et al. Radar: the Cassini Titan radar mapper. *Space Sci. Rev.* **115**, 71–110 (2004).
38. Stiles, B. W. et al. Determining Titan surface topography from Cassini SAR data. *Icarus* **102**, 584–598 (2009).
39. Barnes, J. W. et al. Global-scale surface spectral variations on Titan seen from Cassini/VIMS. *Icarus* **186**, 242–258 (2007).
40. Rodriguez, S. et al. Global mapping and characterization of Titan's dune fields with Cassini: correlation between RADAR and VIMS observations. *Icarus* **230**, 168–179 (2014).
41. Mastrogiuseppe, M. et al. The bathymetry of a Titan sea. *Geophys. Res. Lett.* **41**, 1432–1437 (2014).
42. Hayes, A. G. et al. Hydrocarbon lakes on Titan: distribution and interaction with a porous regolith. *Geophys. Res. Lett.* **35**, 9204 (2008).
43. Malaska, M. J. et al. Identification of karst-like terrain on Titan from valley analysis. *Lunar Planet. Sci. Conf.* **41**, abstr. 1544 (2010).
44. Neish, C. D. & Lorenz, R. D. Titan's global crater population: a new assessment. *Planet. Space Sci.* **60**, 26–33 (2012).
45. Soderblom, J. M. et al. Geology of the Selk crater region on Titan from Cassini VIMS observations. *Icarus* **208**, 905–912 (2010).

## Acknowledgements

Part of this work was conducted at the Jet Propulsion Laboratory (JPL), California Institute of Technology (Caltech), under contract with NASA. This research was supported in part by the Cassini-Huygens mission, a cooperative endeavour of NASA, the European Space Agency and Agenzia Spaziale Italiana managed by JPL/Caltech under a contract with NASA. This research was supported in part by the NASA Astrobiology Institute through its JPL-led team entitled 'Habitability of Hydrocarbon Worlds: Titan and Beyond' and the Cassini Data Analysis Program (grant number NN13D466T to R.M.C.L.). D.A.W. was supported through a grant from NASA's Outer Planets Research Program (grant number NNX14AT29G). A.L.G. was supported by the Institut Universitaire de France.

## Author contributions

R.M.C.L. led the work and wrote the paper. M.J.M., A.M.S., T.V. and M.F. carried out the mapping. A.S. carried out the VIMS analysis and advised on the writing up of VIMS results. A.L.G. advised on interpretation and wrote part of the radiometry results. A.G.H. and S.P.D.B. provided the projected data for the mapping and advised on interpretation. J.R. and S.D.W. advised on interpretation of radar units. E.P.T. advised on the interpretation of ISS data. The Cassini RADAR team acquired and processed the data.

## Additional information

**Correspondence and requests for materials** should be addressed to R.M.C.L.

**Peer review information** *Nature Astronomy* thanks Jason Soderblom and the other, anonymous, reviewer(s) for their contribution to the peer review of this work.

**Reprints and permissions information** is available at [www.nature.com/reprints](http://www.nature.com/reprints).

**Publisher's note** Springer Nature remains neutral with regard to jurisdictional claims in published maps and institutional affiliations.

© The Author(s), under exclusive licence to Springer Nature Limited 2019